Circularly Polarized Aperture-Coupled Circular Microstrip Patch Antennas for L-Band Applications

Nemai C Karmakar, *Member, IEEE*, and Marek E. Bialkowski, *Senior Member, IEEE*

***Abstract*— Circularly polarized aperture-coupled circular microstrip patch antennas are investigated with the goal of obtaining an 8% impedance and ellipticity bandwidth in L-band. Three varieties—a single-feed patch with perturbation segments, a single-feed stacked patch with perturbation segments, and a dual-feed patch with a 3-dB branch line coupler as an external polarizer are considered to obtain the required performance. All the three investigated patch configurations meet the impedance bandwith requirement, but only two varieties: the single-feed stacked patch and the dual-feed patch meet the required ellipticity bandwidth. These antennas feature more than 9-dBi gain. They use low-cost substrates and foam for bandwidth enhancement and, hence, they are attractive for applications where the production cost is of importance.**

***Index Terms*— Circular polarization, patch antennas.**

I. Introduction

RECENT years have seen an enormous expansion of telecommunications services in the L-band frequencies in areas such as mobile satellite, terrestrial cellular, and personal communications systems [1]–[3]. In these systems, antennas play a vital role in obtaining the communication link between a base station (or a satellite) and a mobile unit. Many of these systems require low-profile, low-cost, and low-weight circularly polarized antenna elements to operate over a bandwidth of approximately 10%. In this case, the bandwidth is defined with respect to both impedance and ellipticity (axial ratio). The impedance bandwidth is defined as a range of frequencies over which the input return loss is not smaller than a designated value, usually 10 dB, while the axial ratio bandwidth is defined as a range of frequencies over which the axial ratio (the ratio of major to minor axis of polarization ellipse) does not exceed a designated value, usually 3 dB. Fulfilling these requirements simultaneously can be attempted using microstrip patch antenna technology.

Getting a 10% impedance bandwidth with microstrip elements has been a challenge for some time. However, this problem is now solved, resulting in patch antenna designs meeting approximately a 40% impedance bandwidth [4]. Obtaining an equivalent ellipticity bandwidth has not been covered that well, as it is a more challenging task. It involves not only increasing the patch height above the ground plane, as is the case in impedance bandwidth enhancement for linearly polarized patches, but it also requires optimization of the polarizing elements.

The most elegant configuration for bandwidth enhancement is an aperture (or slot)-coupled microstrip patch antenna (ACMPA) [5], [6]. This configuration not only preserves a fully planar form, but it also eliminates the forward residual radiation of the feeding structure, which is encountered, for example, with edge-fed patches.

In this paper, bandwidth enhancement methods are presented for single-feed and dual-feed ACMPA's operating in L-band. The designs are specifically demonstrated for applications in fixed-beam and phased arrays for use with the Australian Mobilesat™ System [2], which requires circularly polarized antennas operating over a bandwidth of approximately 8%. The presented designs can easily be extended to other L-band satellite and terrestrial systems that require circularly polarized antennas operating over a similar bandwidth.

II. Antenna Configurations and Design Procedures

For the Australian L-band Mobilesat™ carrier Optus B satellites, which use right-hand circularly polarized signals, the receive frequency band is 1545–1559 MHz and the transmit frequency band is 1646–1661 MHz. It is apparent that to cover transmit and receive frequencies, the antenna has to feature an impedance and ellipticity bandwidth of approximately 8% (120 MHz) at a centre frequency of 1.6 GHz.

A. Methods of Obtaining Circular Polarization

Methods of obtaining circular polarization for a microstrip patch are generally divided into two categories [7], [8], one using a dual feed with an external polarizer (for example a Y-junction or a quadrature hybrid) and the other using a single feed and perturbation segements, which are applied to the patch's boundary. These antennas may be required to operate in stand-alone or array configurations. It has to be noted that in fixed-beam arrays, the use of circularly polarized elements to obtain circular polarization is not mandatory. For example, circular polarization can be obtained by arraying linearly polarized elements using a sequential rotation method [9]. In this case, good ellipticity is obtained in the boresight direction. This concept is difficult to extend to variable or steerable beam antenna systems that require circular polarization in off-boresight directions. In such cases, a more suitable solution is to have all the elements in the array being circularly polarized.

Manuscript received December 27, 1995; revised October 14, 1998. This work was supported by the Australian Research Council.

N. C. Karmakar is with the School of Electrical and Electronic Engineering, Nanyang Technological University, Singapore 639798.

M. E. Bialkowski is with the Department of Computer Science and Electrical Engineering, The University of Queensland, Queensland, 4072 Australia.

Publisher Item Identifier S 0018-926X(99)04844-9.

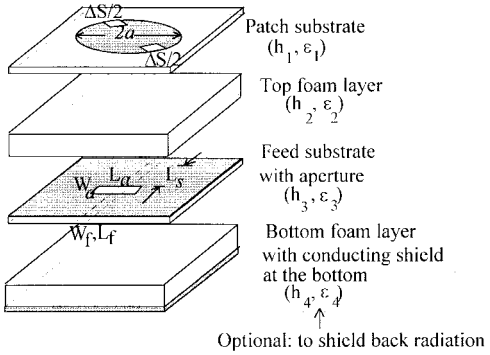

Fig. 1. Configuration of a single feed aperture-coupled circular patch (SF-ACCP) antenna with perturbation segments.

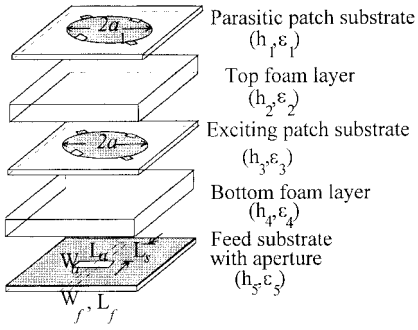

Fig. 2. Configuration of a single-feed aperture-coupled stacked circular patch (SF-ACSCP) antenna with perturbation segments.

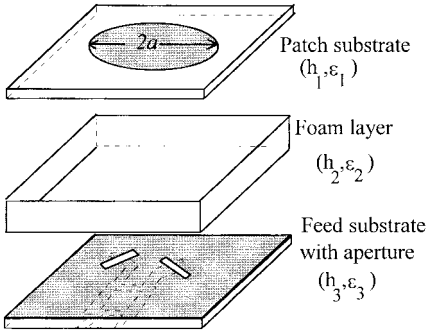

Fig. 3. Configuration of a dual-feed aperture-coupled circular patch (DF-ACCP) antenna.

In order to have a steerable beam array, a beam forming network is required [10]. However, to avoid grating lobes adjacent antenna elements spacing should not exceed a free-space wavelength [11]. Due to this constraint, the beam-forming network competes with antenna feeding elements for available space. This may lead to conflict with some antenna configurations that require extra space in the feed layer to enhance bandwidth performance.

B. Antenna Configurations

Three configurations of aperture-coupled antenna are chosen for the present investigations. These are shown in Figs. 1–3 and include:

1) single-feed aperture-coupled circular patch (SF-ACCP) with perturbation segments;
2) single-feed aperture-coupled stacked circular patch (SF-ACSCP) with perturbation segments;
3) dual-feed aperture-coupled circular patch (DF-ACCP).

The following sections present the designs of these three ACMPA elements. The design goal is to obtain the specified impedance and ellipticity bandwidth (8% at 1.6 GHz), and final verification of the gain bandwidth.

1) SF-ACCP with Perturbation Segments Fig. 1 shows a single-feed aperture-coupled circular patch with perturbation segments. The patch of diameter $2a$ is etched on substrate with height h_1 and dielectric constant ε_1. In order to increase the operational bandwidth, the patch height above the ground plane is increased by including a foam layer of thickness h_2 and dielectric constant ε_2. The patch is fed from an aperture of width W_a and length L_a, which is etched on another substrate with thickness h_3 and dielectric constant ε_3. The feedline of length L_f and width W_f is etched on the bottom side of this substrate. In order to obtain a suitable impedance match, an open-circuited stub of length L_s is used. To generate circular patch radiating fields, perturbation segments with area $(\Delta S/2)$ are etched at the patch edge. These segments are positioned at 45° and 225° with respect to the feedline. To suppress the backward radiation from the aperture, another foam layer with a conducting shield at its bottom can be used. The inclusion of this layer is optional. The reason is that it increases the total volume of the antenna element, which may be found inconvenient in some applications requiring a low-profile antenna. Extra care has to be taken while introducing this back shield. Its usual position is $\lambda/4$ from the aperture plane.

The essential steps, which are used in the design of this antenna element, are given as follows. For the patch excited in the dominant TM_{110} mode, the patch radius is determined using the effective radius a_e [12] of the open-circuited radial resonator model. In the present case, the resonator is filled with a composite dielectric whose effective dielectric constant $\varepsilon_{\mathrm{eff}}$ is calculated according to (1) [13]

$$\varepsilon_{\mathrm{eff}} = \frac{h_1 + h_2}{h_1/\varepsilon_1 + h_2/\varepsilon_2}. \tag{1}$$

The aperture dimensions and the feedline length are assumed to be variable parameters and are selected to obtain an optimal antenna performance. Here, their initial values are chosen as follows: aperture length $L_a = \lambda/10$; width $W_a = \lambda/60$; and stub length $L_s = 10$ mm. The dimensions of segmentation are chosen following the procedure of Heneishi and Suzuki [7].

2) SF-ACSCP with Perturbation Segments In order to improve the operational bandwidth of the patch antenna configuration 1), another patch and another foam layer, as shown in Fig. 2, is added. The added patch, called a parasitic patch, is of diameter $2a_1$ with substrate of height h_1 and dielectric constant ε_1. The other dimensions are as shown in Fig. 2. The new antenna configuration is known as a *stacked-patch* configuration.

The diameters of the two patches and their perturbation segments are determined using a design procedure similar to that

for a single aperture feed single circular patch configuration, which was discussed above. The height of the top foam layer is adjusted to obtain an optimum aperture coupling.

3) DF-ACCP Antenna An alternative configuration to increase the operational bandwidth (both impedance and axial ratio bandwidth) of an aperture-coupled antenna is shown in Fig. 3. In this configuration, two orthogonal apertures and a 3-dB branch line hybrid coupler are used as the feed network. To obtain circular polarization, the slots are orthogonal to each other and are excited by the two open ended output ports of the coupler. In order to increase the operational bandwidth of this type of antenna, a foam layer is used as in the previous configurations.

The patch radius is determined using a procedure analogous to the one for a single-feed patch. The branch line coupler is designed to obtain an amplitude balance overlap in the frequency band between 1545–1661 MHz. A commercial software package such as HP-EEsof Touchstone™ [14] can be used to obtain the design of this coupler.

In the dual-feed aperture-coupled patch design, it is important to obtain a high isolation between the two feedlines. The reason is the operation of the coupler ensures that the two orthogonal modes under the patch are in quadrature, resulting in almost ideal circular polarization of the radiated wave. If this requirement is not met, the connecting of the coupler to the two feedlines results in a very poor axial ratio of this antenna. In the present case, the orthogonal slots are designed to obtain high isolation between the two orthogonal feedlines, in the range of 20 dB or more.

III. Results

A number of antennas, based on the three basic configurations of aperture-coupled microstrip patch antennas 1), 2), and 3) for operation over the Australian Mobilesat™ frequency band were designed, built, and tested. The design parameters included: stub length, aperture dimensions, foam layer thickness, perturbation segment dimensions, and patch radius. Two approaches—one based on the use of the commercial software, Ensemble™ from Boulder Technologies [15], and the other relying on experimental testing—were employed in the design process. During the use of Ensemble™, a significant discrepancy was encountered between computed and experimental results for the axial ratio of perturbation segmented patches. It was discovered that this discrepancy was due to the narrow grid of the perturbation segments, which led to singularities in the Ensemble™ simulation engine. For this reason, the results obtained with Ensemble™ were discarded and the final design of the perturbation segmented single and stacked patches relied on the experimental approach. Due to the same reason, only experimental results are presented here.

During the initial phase of the design process it was found that the open stub length had a secondary influence on impedance bandwidth for all the investigated configurations. In contrast to the stub length, the aperture length and the thickness of the foam layer had a considerable effect on the operational bandwidth. The use of the foam layer not only contributed to an increase in the antenna's operational bandwidth, but it also helped to avoid spurious resonances due to air gaps between the layered substrates when the foam was absent. Detailed results for the three types of aperture-coupled antennas are presented in the following sections.

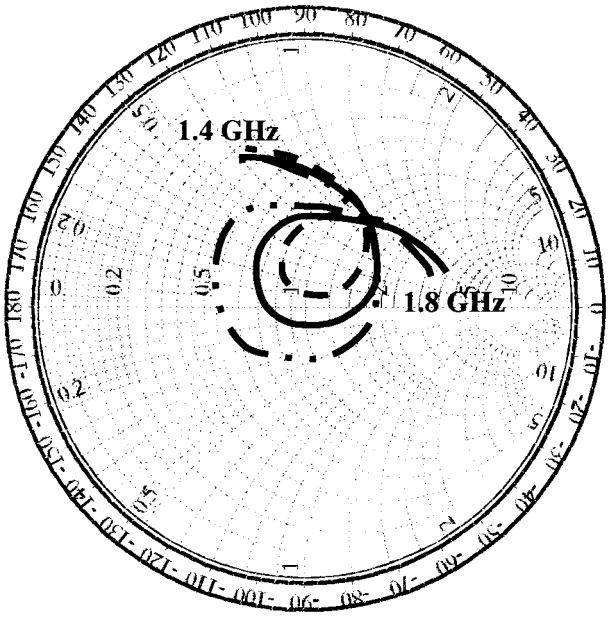

Fig. 4. Smith chart plots of input impedance showing the effect of aperture dimensions on the input impedance match of an ACMPA. Dashed line (- - -) for $W_a \times L_a = 21.75$ mm $\times$ 3.7 mm, solid line (——) for $W_a \times L_a = 23.45$ mm $\times$ 3.7 mm, and dashed-dotted line (— - - —) for $W_a \times L_a = 27.45$ mm $\times$ 3.7 mm. Other dimensions are as shown in Table I for a 3-mm foam layer.

A. SF-ACCP with Perturbation Segments

1) Input Impedance The experimental investigations were commenced with the single aperture-feed circular-patch configuration of Fig. 1. The substrate material used in the experiments was RT/Duroid 5880 with thickness $h = 0.785$ mm and a relative dielectric constant $\varepsilon_r = 2.2$. The foam layer had a relative dielectric constant $\varepsilon_{r2} = 1.47$. In the initial stage, foam with thickness $h_2 = 3$ mm was used. In this case, the calculated effective dielectric constant, using (1), was $\varepsilon_{\text{eff}} = 1.87$ and the resulting patch radius was 40.15 mm. The initial area of the perturbation segment $(\Delta S/2)$ was taken as 6 mm $\times$ 4 mm and the initial aperture dimensions were 20.5 mm $\times$ 3.7 mm.

The aperture length was varied to obtain the maximum impedance bandwidth. The corresponding Smith Chart impedance plots are shown in Fig. 4. The experiments were performed for three aperture lengths of 21.75 mm, 23.45 mm, and 27.45 mm. The maximum input impedance bandwidth of 73.3 MHz was achieved for the aperture with dimensions 27.45 mm $\times$ 3.7 mm.

Note that the length of the aperture had a significant effect on the antenna's matching condition. This was in contrast to the aperture width variations (within reasonable limits of about $\lambda/20$ [4]), which had an insignificant effect on the impedance bandwidth.

TABLE I
VARIATIONS OF RESONANT FREQUENCY AND INPUT-IMPEDANCE BANDWIDTH WITH FORM LAYERS AND APERTURE DIMENSIONS. THE PATCH RADIUS $a = 40.15$ mm, $\varepsilon_{r1} = \varepsilon_{r3} = 2.2$, $h_1 = h_3 = 0.875$ mm, $\varepsilon_{r2} = 1.47$, $L_s = 10$ mm, $W_f = 2.43$ mm, $L_f = 55$ mm, $\Delta S/2 = 10$ mm $\times$ 5 mm

Foam layer h_2 = 3 mm			Foam layer h_2 = 8.5mm		
Aperture dimensions (mm × mm)	10-dB RL bandwidth (MHz)	Resonant frequency (MHz)	Aperture dimensions (mm × mm)	10-dB RL bandwidth (MHz)	Resonant frequency (MHz)
20.5× 3.7	0	1765	27.5 × 5	0	1666
21.75×3.7	53.3	1756	30.15 × 5	53.3	1660
23.45 × 3.7	66.7	1623	32.0 × 5	120	1650
27.45 × 3.7	73.3	1600	32.8 × 5	150	1646
Over coupled with increase of aperture dimensions			34.8 × 5	156	1642
			35.2 × 5	180	1635

Due to the fact that the achieved impedance bandwidth for the 3-mm thick foam was approximately half of the required bandwidth (only 60 MHz against the required 120 MHz), the next experiments involved a thicker foam layer with height $h_2 = 8.5$ mm. The experimental results for both cases (3.7-mm foam and 8.5-mm foam) are summarized in Table I. As seen in this table, the impedance bandwidth of 180 MHz was achieved with aperture dimensions of 35.2 mm $\times$ 5 mm and the 8.5-mm thick foam layer.

The information in Table I concerning the behavior of input-impedance bandwidth and design (resonant) frequency as a function of aperture length and foam layer thickness is illustrated in the graphical form in Fig. 5(a) and (b). From the two graphs it can be inferred that both the aperture length and the thickness of the foam layer govern the input impedance bandwidth. The resonant frequency becomes less sensitive to the aperture length for a thicker foam layer.

2) Axial Ratio Versus Perturbation Segments Having achieved an impedance bandwidth exceeding the required 120 MHz, the next experiments with a single aperture-feed circular patch concerned the effect of perturbation segments on the axial ratio bandwidth. The axial ratio measurements were initially taken at a single frequency of 1.660 GHz using a spinning dipole on the boresight axis of the ACMPA. In order to minimize the effect of the perturbation segments on the resonant frequency, similar size extruded and intruded segments were etched in the patch.

Table II shows the measured results for the axial ratio of the single aperture-feed single circular-patch antenna.

It can be seen in this table that with an increase in the segmentation area, the axial ratio is improved. An axial ratio of 2.0 dB is achieved with segmentation dimensions of 10 mm $\times$ 8 mm.

A relationship between the axial ratio and the ratio of the total segmentation area $(\Delta S/S)$, where $S = \pi a^2$ is the area of the circular patch, is shown in Fig. 6. As can be seen in this figure, the axial ratio decreases exponentially with the total area of the perturbation segmentation on the patch. A reasonably good axial ratio of 2 dB is achieved when the segmentation ratio is 5%.

3) Return Loss and Axial Ratio Bandwidth Having obtained an ellipticity of less than 2 dB at the center design frequency of 1.6 GHz, the next steps included axial ratio measurements over the entire Mobilesat™ frequency band of 1.545–1.661 GHz. During these experiments, the foam thickness was further increased from 8.5 to 11.2 mm. This time the ACMPA produced a good match with aperture dimensions of 40.5 mm$\times$ 6 mm. The maximum return loss was 31 dB at 1.55 GHz and the 10-dB return-loss bandwidth was approximately 260 MHz. This was for the case when the dimensions of both intruded and extruded segments were increased to 14.2 mm $\times$ 9.7 mm.

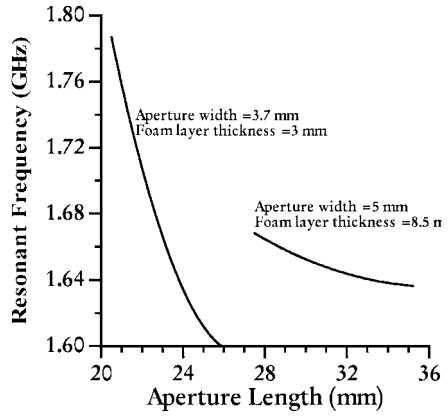

(a)

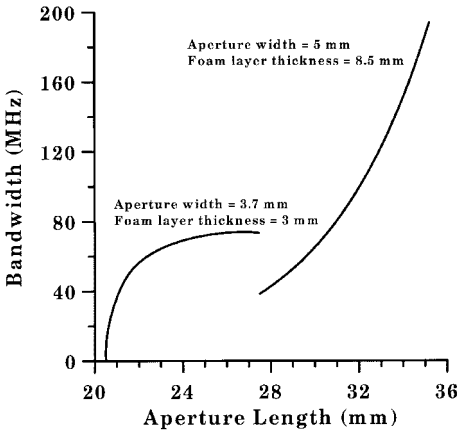

(b)

Fig. 5. (a) Bandwidth versus aperture length plots. (b) Resonant frequency versus aperture length of a single-feed single-patch aperture-coupled patch antenna with foam thickness and aperture width as parameters. Other antenna parameters were: $a = 40.15$ mm, $\varepsilon_1 = \varepsilon_3 = 2.2$, $h_1 = h_3 = 0.875$ mm, $\varepsilon_2 = 1.47$, $L_s = 10$ mm, $W_f = 2.43$ mm, $L_f = 55$ mm, $\Delta S/2 = 10$ mm $\times$ 5 mm.

TABLE II
VARIATION OF AXIAL RATIO OF A SINGLE APERTURE-FEED CIRCULARLY POLARIZED CIRCULAR-PATCH ANTENNA WITH THE PERTURBATION SEGMENTATION AREAS MEASURED AT 1.6 GHz. THE DIMENSIONS ARE AS FOR TABLE I FOR 8.5-mm-THICK FOAM LAYER

Intruded Segments Area (mm^2)	Extruded Segments Area (mm^2)	Axial ratio = P_{max}-P_{min} (dB) (by 360° Dipole Rotation)
6×3	0×0	25
6×5	0×0	19
8×6	0×0	12
8×6	8×6	7.5
10×8	8×6	5.5
10×8	10×8	2

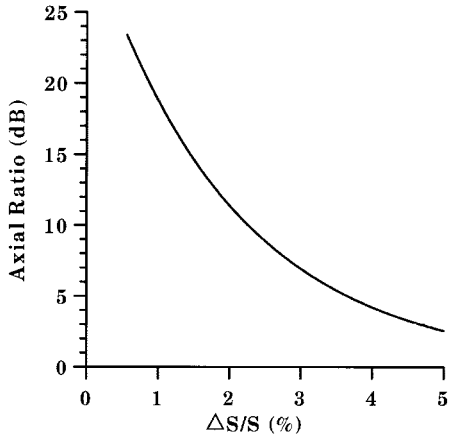

Fig. 6. Axial ratio versus segmentation area ratio $(\Delta S/S)$ for a single-feed perturbation-segmented aperture-coupled patch antenna at 1.6 GHz. The antenna dimensions are as for Table I.

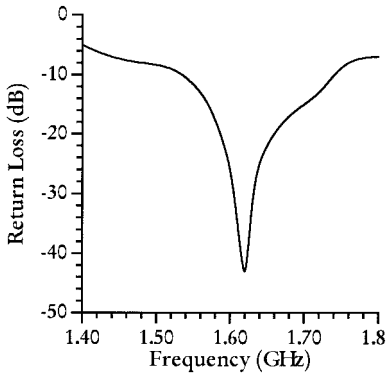

(a)

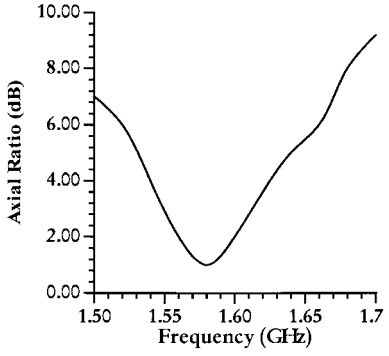

(b)

Fig. 7. Bandwidth of a single-feed perturbation-segmented patch. (a) Return-loss bandwidth. (b) AR bandwidth. The ACMPA dimensions: $a = 40.15$ mm, $\Delta S^{+}/2 = \Delta S^{-}/2 = 14.2$ mm$\times 9.8$ mm, $h_1 = 0.785$ mm, $\varepsilon_1 = 2.2$, $h_2 = 11.2$ mm, $W_a = 6$ mm, $L_a = 41$ mm, $L_s = 10$ mm, $W_f = 2.43$ mm, $L_f = 55$ mm.

The plots of return loss and axial ratio versus frequency are shown in Fig. 7(a) and (b), respectively. It is seen there that the 3-dB axial ratio bandwidth is only 60 MHz, which is about 23% of the return-loss bandwidth.

Due to the difficulty to obtain the required ellipticity bandwidth even when using a considerably thick (12 mm) composite substrate, a stacked configuration with perturbation segments was considered next.

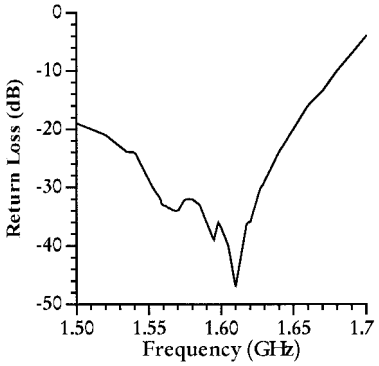

(a)

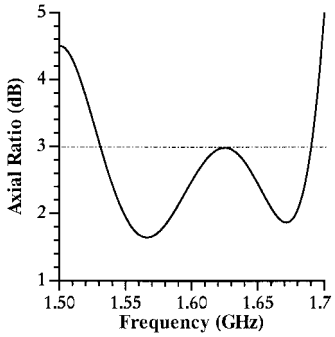

(b)

Fig. 8. Input impedance and axial ratio for a single-feed stacked-patch antenna. (a) Measured return loss. (b) Measured axial ratio. The ACMPA dimensions: parasitic patch $a_1 = 39.45$ mm, $\Delta S^{+}/2 = 10 \times 7$ mm^2, $\Delta S^{-}/2 = 14.2 \times 9.8$ mm^2, $h_1 = 0.785$ mm, $\varepsilon_1 = 2.2$, exciting patch $a = 40.15$ mm, $\Delta S^{+}/2 = \Delta S^{-}/2 = 14.2 \times 9.8$ mm^2, $h_3 = 0.785$ mm, $\varepsilon_3 = 2.2$, top foam layer $h_2 = 11.2$ mm, aperture $W_a = 6$ mm, $L_a = 41$ mm,feedline $L_s = 10$ mm, $W_f = 2.43$, $L_f = 55$ mm.

B. SF-ACSCP with Perturbation Segments

1) Return-Loss and Axial-Ratio Bandwidth The top patch was made slightly smaller than the bottom one so that the two patch resonances could become additive to improve the operational bandwidth. The top patch of radius 39.45 mm and the bottom patch of radius 40.15 mm were etched on the same substrate material RT/Duroid 5880: $h = 0.785$ mm and $\varepsilon_r = 2.2$. They were separated by a foam layer of thickness 6 mm. The bottom foam layer thickness between the bottom patch and the aperture ground plane was chosen to be 9 mm. The aperture dimensions were 44 mm $\times$ 8 mm.

Fig. 8(a) and (b) shows the measured results for the return loss and axial ratio. The return loss bandwidth is 350 MHz and the axial ratio bandwidth is approximately 150 MHz. These results show that similarly as for a single patch with perturbation segments the ellipticity bandwidth is only 23% of the return-loss bandwidth. Nevertheless, the developed antenna meets impedance and ellipticity bandwidth for the Australian Mobilesat™.

2) Radiation Patterns and Gain In order to complete the design process, the stacked-patch antenna was tested with respect to its radiation pattern and gain. The measured radiation patterns including the effect of a back shield, situated at about $\lambda/4$ away from the aperture ground plane, are shown in Fig. 9(a), while the gain measured against the standard dipole

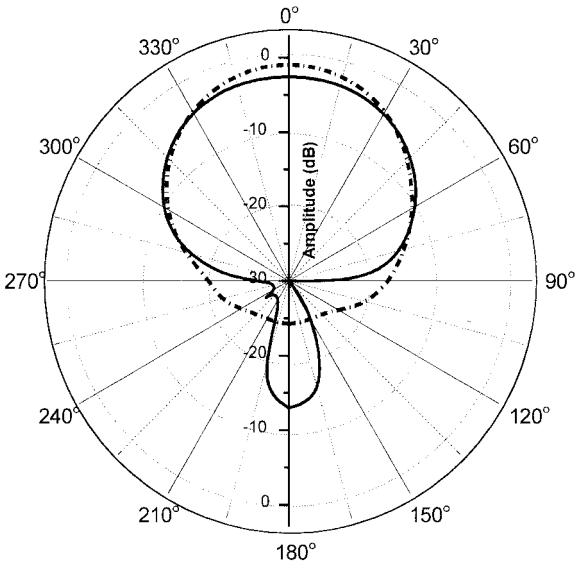

(a)

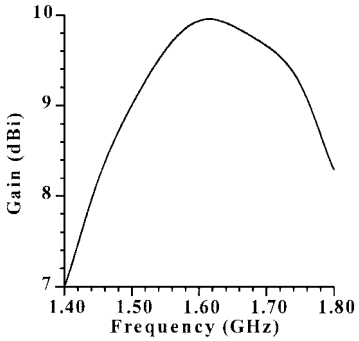

(b)

Fig. 9. Measured radiation pattern of a single-feed stacked-patch antenna. (a) Radiation patterns at 1.6 GHz, solid line (——) antenna without back shield, dashed-dotted line (— - —) antenna with a back shield; (b)Gain. The dimensions are as for Fig. 8.

gain is presented in Fig. 9(b). It can be seen that without the shield, there is significant backward radiation with a backlobe level of 13 dB below the main lobe peak. With the shield, the backward radiation is reduced to 25 dB down from the peak value. The use of the shield enhances the antenna gain by approximately 1 dB. The half-power beamwidth for both cases is 62.4°. The result presented in Fig. 9(b) shows that the ACMPA has a gain of 9.5 dBi at 1545 MHz and 9.8 dBi at 1660 MHz.

C. DF-ACCP Antenna

Finally, the dual-fed circularly polarized ACMPA of Fig. 3 was designed, built, and tested. The design resulted in a patch with a radius of 42 mm, a 9-mm-thick foam layer, and an aperture with width $W_a = 4$ mm and length $L_a = 39$ mm. Isolation of better than 20 dB between the orthogonal feeds and a return loss of better than 10 dB for individual feeds were aimed at before connecting a 3-dB coupler.

1) Isolation Between Feedlines and Axial Ratio In order to obtain the required design objectives, slot separations of 20 mm and 25 mm (distance between the nearest corners of

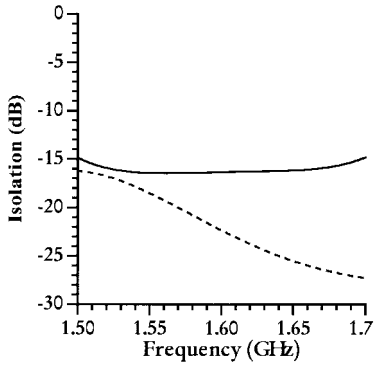

(a)

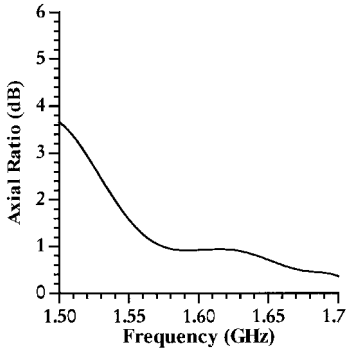

(b)

Fig. 10. (a) Isolation. (b) Axial ratio of a dual feed aperture-coupled patch antenna: $a = 42$ mm, $h_1 = 0.785$ mm, $\varepsilon_1 = 2.2$, $h_2 = 9$ mm, $\varepsilon_2 = 1.47$, aperture dimensions, $L_a = 39$ mm, $W_a = 4$ mm, stub length $L_s = 10$ mm. Solid line (——) for $d = 20$ mm and dashed line (- - - - -) for $d = 25$ mm.

orthogonal rectangular apertures) were chosen. The measured results for the two separations are shown in Fig. 10(a). It is seen that the greater isolation is obtained with a larger separation of apertures. Hence, the configuration with the 25-mm slot separation was chosen for the final antenna development. For this slot arrangement, a 3-dB branch line coupler was added and axial ratio measurements versus frequency were taken. The results of these measurements are shown in Fig. 10(b). Note that in this case, the patch diameter was adjusted to 86 mm to achieve the correct resonant frequency.

It is seen that the antenna features axial ratios of 1.69 dB at 1545 MHz and 0.6 dB at 1661 MHz. By comparing the behavior of curves in Fig. 10(a) and (b), it can be seen that the ellipticity characteristic follows the isolation characteristic.

2) Gain In order to complete the design, gain measurements were also taken. The measured gain results are shown in Fig. 11. It is seen that the developed antenna features a gain of 9.75 dBi at 1545 MHz and 8.6 dBi at 1661 MHz.

D. Comparison Between Single- and Dual-Feed Aperture-Coupled Patch Antennas

By comparing the results for the single aperture-feed stacked-patch antenna and the dual aperture-feed single-patch antenna, it can be deduced that the two developed antennas feature similar gain performance. However, in terms of the quality of circular polarization, the dual-feed aperture-coupled patch shows a superior performance. This is due to an external

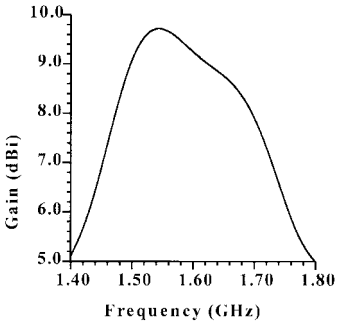

Fig. 11. Gain versus frequency for a dual-feed circularly polarized ACMPA; dimensions are as for Fig. 10.

polarizer, which ensures an ideal quadrature excitation of the two modes contributing to circular polarization. This is under the condition that the isolation between the two feedlines are sufficiently high (20 dB or more). However, one inconvenience of this configuration is that it reduces the available space for the beamforming network [16]. This is due to the use of an external polarizer in the form of a 3-dB branch line coupler. At 1.6 GHz, this hybrid is 35 mm $\times$ 35 mm in size and, hence, it takes more area than is available under the patch. This is found unattractive when this element is to be employed in a phased array as it leaves only a small space between adjacent antenna elements to include phase shifting modules. In contrast to the dual-feed patch, the single aperture-coupled patch leaves about double the area under the patch to include a phase shifter. Hence, this element may be a preferable choice in a phased-array antenna [16].

IV. Conclusion

Three configurations of a circularly polarized aperture-coupled patch antenna with single- and dual-feed arrangements for use in L-band communications systems requiring approximately 8% impedance and axial ratio bandwidth, have been investigated. Two methods for obtaining circular polarization have been considered: 1) using a single feedline and a patch with perturbation segments and 2) a dual-feed patch with orthogonal apertures and a branch line coupler. The effects of the aperture length, foam layers, and the perturbation segmentation on the impedance and axial ratio bandwidth have been analyzed. It has been found that for a single-feed aperture-coupled patch antenna configuration the axial ratio bandwidth is only 23% of the return-loss bandwidth. Due to this constraint, this antenna is unable to deliver the required ellipticity bandwidth even with very thick foam layers, which produce about 15% impedance bandwidth. The required impedance and ellipticity bandwidth can, however, be obtained by introducing a second patch and by modifying the structure to a stacked-patch configuration. An alternative way to obtain the required impedance and ellipticity bandwidth is to use a dual-aperture arrangement with an external polarizer in the form of a 3-dB branch line coupler.

The last two antenna elements feature the desired impedance and axial ratio bandwidth in addition to 9-dBi gain across the specified band. The dual-feed patch offers a better axial ratio. However, this performance is achieved at the expense of the extra space taken by an external polarizer in the feed network layer. This solution may be found unattractive in a phased-array design, where the space for the beamforming network is often at a premium. In such cases, the single-feed aperture-coupled stacked patch can be a preferable option.

References

[1] W. W. Wu, E. F. Miller, W. L. Pritchard, and R. L. Pickholtz, "Mobile satellite communications," *Proc. IEEE*, vol. 82, pp. 1431–1448, Sept. 1997.
[2] B. R. Elbert, *The Satellite Communication Applications Handbook*. Norwood, MA: Artech House, 1997.
[3] B. Miller, "Satellites free the mobile phone," *IEEE Spectrum*, vol. 35, no. 3, pp. 26–35, Mar. 1998.
[4] D. M. Pozar, "A review of aperture coupled microstrip patch antennas: History, operation, development, and applications," http:\\www.rfglobnet.com., pp. 1–12.
[5] P. L. Sullivan and D. H. Schaubert, "Analysis of an aperture-coupled microstrip antenna," *IEEE Trans. Antennas Propagat.*, vol. AP-34, pp. 977–984, Aug. 1986.
[6] D. M. Pozar, "A reciprocity method of analysis for printed slot and slot-coupled microstrip antennas," *IEEE Trans. Antennas Propagat.*, vol. AP-34, pp. 1439–1446, Dec. 1986.
[7] M. Haneishi and Y. Suzuki, "Circular polarization and bandwidth," *Handbook of Microstrip Antennas*, J. R. James and P.S. Hall, Eds. London, U.K.: Peter Peregrinus, 1989, vol. 1, ch. 4, pp. 219–274.
[8] M. I. Aksun, Z. H. Wang, S. L. Chuang, and Y. T. Lo, "Double-slot-fed microstrip antennas for circular polarization operation," *Microwave Opt. Technol. Lett.*, vol. 2, no. 10, pp. 343–346, Oct. 1989.
[9] J. Huang, "A technique for an array to generate circular polarization with linearly polarized elements," *IEEE Trans. Antennas Propagat.*, vol. AP-34, pp. 1113–1119, Sept. 1986.
[10] R. P. Owens, "Chapter 14 microstrip antenna feeds," *Handbook of Microstrip Antennas*, J. R. James and P. S. Hall, Eds. London, U.K.: Peter Peregrinus, 1989, vol. 2, pp. 815–870.
[11] C. A. Balanis, *Antenna Theory: Analysis and Design*. New York: Wiley, 1997.
[12] I. J. Bahl and P. Bhartia, *Microstrip Antennas*. Dedham, MA: Artech House, 1980.
[13] R. F. Harrington, *Time Harmonic Electromagnetic Fields*. New York: McGraw-Hill, 1961.
[14] EEsof Series IV Touchstone™ User's Guide, vols. 1, 2, Feb. 1993.
[15] *Boulder Microwave Technologies, Inc.*, ENSEMBLE® Version 5.0, www.bmt.com.
[16] N. C. Karmakar and M. E. Bialkowski, "Designing an L-band phased-array antenna for mobile satellite communications," in *Proc. Asia-Pacific Microwave Conf.*, Hong Kong, China, Dec. 1997, pp. 949–952.

Nemai C. Karmakar (M'99) was born in Satkhira, Bangladesh, in 1963. He received the B.Sc. and M.Sc. degrees in electrical and electronic engineering from Bangladesh University of Engineering and Technology, Dhaka, Bangladesh, the M.Sc. degree (electrical engineering) from the University of Saskatchewan, Canada, and the Ph.D. degree from the University of Queensland, Brisbane, Australia, in 1987, 1989, 1991, and 1999, respectively.

He worked as an Assistant Engineer in the Electronics Institute, Atomic Energy Research Establishment, Savar, Dhaka, from 1989 to 1990. In August 1990, he was a Research Assistant at the Communications Research Group, University Saskatchewan, Canada. From 1992 to 1995 he worked as a Microwave Design Engineer at Mitec Ltd., Brisbane, Australia, where he contributed to the development of land mobile satellite antennas for the Australian Mobilesat. He worked as a Research Engineer, Radar Laboratory, Nanyang Technological University, Singapore, from 1998 to 1999. He is currently working as an Assistant Professor in the Division of Communication Engineering, Nanyang Technological University. He has published about 30 technical papers, reports, and book chapters. His research interests include broad-band microstrip antennas and arrays, beamforming networks, near-field/far-field antenna measurements, microwave device modeling, and monostatic and bistatic radar.

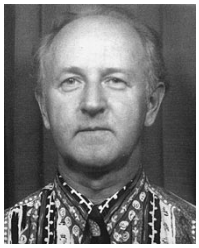

Marek E. Bialkowski (SM'88) received the M.Eng.Sc. (applied mathematics) and Ph.D. (electrical engineering) degrees, both from the Warsaw Technical University, Warsaw, Poland, in 1974 and 1979, respectively.

In 1977, he joined the Institute of Radioelectronics, Warsaw Technical University and in 1979 became an Assistant Professor there. In 1981 he spent one year at the University College Dublin, Ireland, carrying out research in the area of microwave circuits under a postdoctoral research fellowship by the Irish Department of Education. In 1982 he conducted research on electromagnetic models for waveguide diode mounts at the University of Queensland, Brisbane, Australia, under a postdoctoral research fellowship from that university. In 1984 he joined the Department of Electrical and Electronic Engineering, James Cook University, Townsville, Australia, as a Lecturer and then Senior Lecturer in the field of communications. In 1988 he was a Visiting Lecturer in the Department of Electronics and Computer Science, University of Southampton, U.K. In 1989, he joined the Department of Electrical Engineering at the University of Queensland, Brisbane, Australia, where he is the Head of the Microwave/Antenna and Optoelectronics Group. In 1994 he held an appointment as a Visiting Professor in the University of Victoria, Canada. Since 1998 he has held Professorships both at the University of Queensland, Australia and at Nanyang Technological University, Singapore. His research interests include antenna systems for mobile satellite communications, low-profile antennas for reception of satellite broadcast TV programs, conventional and quasi-optical power combining techniques, six-port measurement techniques, industrial applications of microwaves, and computational electromagnetics. He has published extensively in all these areas. His list of publications includes over 200 technical papers and one book.